LC Resonant Circuits Based Matching Networks for Continuous Mode MMIC Power Amplifiers

Yang Xu and Anding Zhu

***Abstract*—This paper presents a practical design methodology to construct output matching networks for broadband continuous mode monolithic microwave integrated circuit (MMIC) power amplifiers (PAs). Unlike conventional harmonic manipulation approaches, combinations of parallel and series *LC* resonant circuits are utilized to build the matching networks as it can generate frequency-dependent components and locate the varying impedance of continuous mode. With a proper design, the impedance variation in frequency domain can be mapped to the frequency response of the matching network at the fundamental frequency and the second harmonic simultaneously. Matching network design procedures are demonstrated and results show that the frequency response of the network has very good approximation with the desired continuous mode conditions. A prototype PA is implemented on 0.25-μm Gallium Nitride (GaN) MMIC process, and tested with both continuous-wave and modulated signals. Measurement results show 50.82% maximum drain efficiency and 8.5 dB gain can be achieved across the operation bandwidth of 5.4 to 6.4 GHz.**

***Keywords*—Broadband, continuous mode, GaN, monolithic microwave integrated circuit (MMIC), power amplifiers**

I. Introduction

With increasing demands for higher data rate and wider signal bandwidth, the broadband power amplifier (PA) with high efficiency is essential in the next generation, i.e., 5G, wireless systems. However, maintaining high efficiency over a wide bandwidth is difficult since bandwidth enhancement is often accompanied with efficiency degradation. The continuous mode PA has shown great potential in broadband PA design [1]. It introduces reactive load to the fundamental and harmonics matching, allowing PA to produce constant output power and maintain the same efficiency over a wide impedance range [2].

Despite many broadband continuous mode PAs have been reported [3][4][5][6], the output matching network design for broadband continuous mode operation is challenging as specific impedance requirements are enforced to guarantee the performance. The existing designs mainly rely on load-pull measurement and mostly are implemented with microstrip lines or filter-based matching networks [7][8][9]. Those discrete circuit design approaches deal with the characteristic impedance transmission lines, and have limited integration potential.

When 5G is evolving towards small cells, Monolithic Microwave Integrated Circuit (MMIC) with compact size is preferred for low power transmitters in dense networks. The MMIC process enables compact circuit design with high power density and reasonable efficiency [10][11][12]. The active devices can be adjusted for purpose, as observed in MMIC Doherty PA designs and multi-stage PA designs [13][14]. Moreover, in the designs involving harmonic manipulation, it is normally fulfilled with additional harmonic termination transmission lines [15][16]. While the commonly used strategies for PCB is no longer effective for MMIC, we need to explore the lumped element based design approach outside the discrete circuits.

LC resonant circuits can provide precise impedance matching but it always involves complex mathematical circuit synthesis and the bandwidth is limited [17][18]. In this paper, a simple design approach utilizing *LC* resonant circuits is proposed to construct broadband continuous mode output matching networks. Different from most matching strategies using lumped components [19], it adopts *LC* resonant circuits not only to locate the harmonic reactance, but more importantly, to generate equivalent frequency-dependent components with different behaviors at the fundamental frequency and second harmonic. Thus, the continuous mode impedance requirements are satisfied in broadband without complicated network synthesis. The lumped component based design procedure is suitable for realistic MMIC implementation.

II. Broadband Continuous Mode Matching network Construction

In the continuous Class-B mode, the fundamental impedance Z_{f0} and second harmonic impedance Z_{2f0} can be expressed as [2]:

$$Z_{f0} = R_{opt} - j\delta R_{opt} \quad (1)$$

$$Z_{2f0} = 0 + j\frac{3\pi}{8}\delta R_{opt} \quad (2)$$

This publication was emanated from research supported in part by research grants from Science Foundation Ireland (SFI) and co-funded under the European Regional Development Fund under Grant Numbers 13/RC/2077 and 16/IA/4449.

The authors are with the School of Electrical and Electronic Engineering, University College Dublin, Dublin 4, Ireland (email: yang.xu@ucdconnect.ie; anding.zhu@ucd.ie).

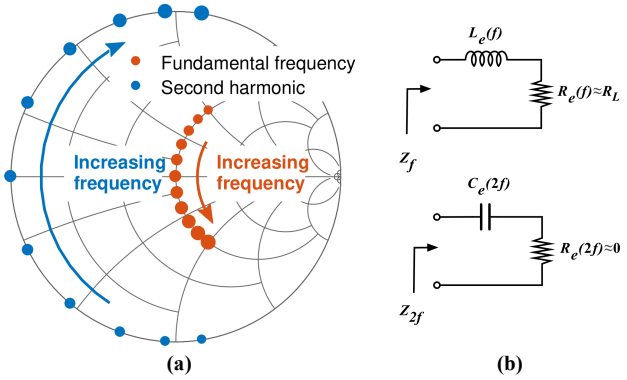

Fig. 1. Broadband continuous Class-B mode operation. (a) δ variation in the frequency domain. (b) The equivalent frequency-dependent components at the fundamental frequency and second harmonic for δ inside [-1,0].

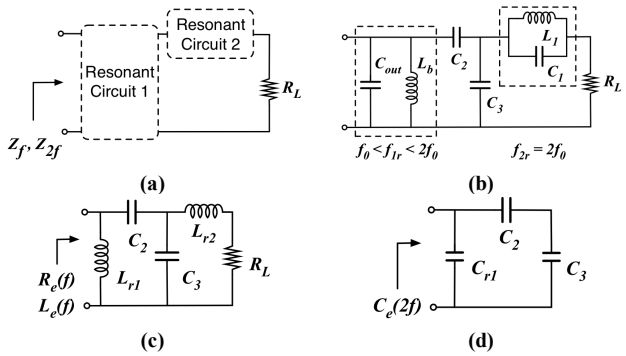

Fig. 2. The matching network construction procedure. (a) The general topology with two *LC* resonant circuits. (b) The proposed circuit structure based on (a). (c) The equivalent circuit at the fundamental frequency. (d) The equivalent circuit at the second harmonic.

where R_{opt} is the optimum load and δ varies in a range of [-1,1]. The continuous mode impedance expands from a single point to a set of solutions, making the bandwidth extension possible. The operation principle is simple but realizing the continuous mode across a wide bandwidth is not easy. It can only be achieved when δ variations are properly mapped to the frequency response variations of the matching network. Specifically, when δ becomes a function of the frequency, the fundamental impedance trajectory variation must follow the opposite direction of that of the second harmonic, as shown in Fig. 1(a). Consequently, for the output matching network, the varying impedances at both frequencies must be converted to the load generated by frequency-dependent components. For instance, when δ stays inside [-1,0], the fundamental load has a positive reactance that equivalent to a frequency-dependent inductor $L_e(f)$, and the negative second harmonic reactance can be viewed as a frequency-dependent capacitor $C_e(2f)$, as shown in Fig. 1(b). Furthermore, the matching network is expected to keep constant fundamental resistance and let the second harmonic resistance stay zero inside the bandwidth. Building such matching networks is challenging.

As we know, a series *LC* circuit acts as a short circuit when resonating, whereas a parallel *LC* circuit acts as an open circuit when resonating. It would behave like a frequency-dependent component when deviating from its resonance frequency. For instance, when the operating frequency is lower than its resonance frequency f_r, the parallel *LC* is equivalent to an inductor and when the operating frequency is higher than f_r, it is equivalent to a capacitor. Take a parallel *LC* resonant circuit for example, when its operation frequency f_0 deviates from its resonance frequency f_r, its equivalent value can be expressed as

$$L_{parallel}(f) = L\left(1-\frac{f_0^2}{f_r^2}\right)^{-1},\ f_r > f_0 \quad (3)$$

$$C_{parallel}(f) = C\left(1-\frac{f_r^2}{f_0^2}\right),\ f_r < f_0 \quad (4)$$

This property is useful when constructing output matching networks for broadband continuous mode. Not only can it generate short or open circuit, but also it can create the frequency-dependent component which can be utilized to model the behavior of $L_e(f)$ and $C_e(2f)$. When combining series and parallel *LC* circuits together, it is possible to construct broadband matching networks that meet continuous mode impedance requirements without going through complex circuit synthesis.

TABLE 1
THE COMPONENT VALUE RANGE AND THE OPTIMAL VALUES

Variable	Value range	Optimal value
f_{1r} (GHz)	[6.50, 7.55]	7.66
L_b (nH)	[2.01, 2.85]	2.06
f_{2r} (GHz)	[9.00, 13.00]	10.41
L_1 (nH)	[0.10, 1.09]	1.07
C_1 (pF)	[0.14, 3.00]	0.22
C_2 (pF)	[0.11, 3.00]	0.31
C_3 (pF)	[0.10, 0.58]	0.21

Fig. 2(a) shows a possible combination with two *LC* units, and one possible circuit structure is proposed in Fig. 2(b). Resonant Circuit 1, including drain bias inductor L_b and output capacitance C_{out}, resonates between the fundamental frequency and the second harmonic. Resonant Circuit 2 whose resonance frequency f_{2r} equals to the second harmonic is placed in series. C_2 is added in between and it can serve as the DC block capacitor. C_3 is placed in parallel to attain better fundamental resistance fitting and larger reactance adjustment range at the second harmonic.

Once chosen the topology, the frequency response of the network can be determined through analyzing the equivalent circuits at both frequencies, shown in Fig. 2(c) and Fig. 2(d), respectively. At the second harmonic, the open circuit created by Resonant Circuit 2 locates the second harmonic load at the edge of the Smith Chart. Resonant Circuit 1 is equivalent to the frequency-dependent component C_{r1}. The behavior of $C_e(2f)$ is mainly decided by C_{r1}, which can be expressed as the function of f_{1r} based on its resonance characteristics. The second harmonic reactance and the corresponding $\delta(2f)$ are functions of f_{1r}, C_2 and C_3. At the fundamental frequency, L_{r1} and L_{r2} are the equivalent frequency-dependent inductors from two resonant circuits. Similarly, L_{r1} is the function of f_{1r}, and L_{r2} has L_{r2}=4/3 L_1 since it resonates at $2f_0$. All those variables jointly model the fundamental load and its corresponding $\delta(f)$. After the desired frequency response is determined, each component

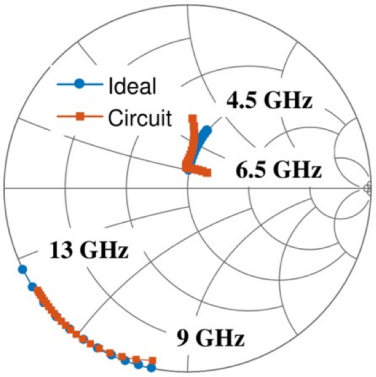

Fig. 3. Simulated frequency response of the proposed circuit and the ideal continuous impedance trajectory inside the same δ range [-0.7, -0.2] with impedance normalized to R_{opt}.

value can be found by using optimization algorithms, e.g., the Bayesian Optimization (BO) in [20]. In this design, the selected transistor has $R_{opt} = 140\,\Omega$ and $C_{out} = 0.21\,pF$, and all component values are limited by the MMIC process. δ is expected to stay inside [-1,0] at operating bandwidth from 4.5 GHz to 6.5 GHz. Objective functions are defined in BO to model the matching network with the target of searching for the optimal fitting. The optimal estimation given by BO are listed in Table 1.

Fig. 3 shows the simulated performance based on the optimal estimation. The fundamental resistance follows R_{opt} very well, especially at lower frequency, whereas it starts to deviate at higher frequency but the discrepancy is still acceptable when it comes to practical applications. The second harmonic resistance locates at the edge of Smith Chart, meaning Resonate Circuit 2 has successfully removed the impact of the load. The predicted optimal δ range is estimated as [-0.7, -0.2], where the behavior of *δ(f)* and *δ(2f)* fit well with the desired impedance trajectory inside the bandwidth. δ varies with increasing frequency in a linear fashion from -0.7 to -0.2 is also presented in the figure for reference.

III. Circuit Implementation and Measurements

The circuit was implemented with 0.25-μm GaN HEMT from WIN Semiconductors, and the transistor with size 4×125 μm was biased at V_D = 28 V and V_G = -2.5 V. The output matching network was designed based on the optimal estimations, and the input matching network was designed based on source pull. The inductors in the proposed circuit structure were replaced with MMIC transmission lines.

The circuit schematic and chip photograph are shown in Fig. 4 (a). The chip size is 2 mm×1 mm and the fabricated chip is mounted on a PCB test fixture with bonding wires for measurement. Continuous wave (CW) measurement results and simulation results are compared in Fig. 4 (b) and Fig. 4(c). Simulation results have taken the parasitic effect, the bonding wire impact and the thermal problem into consideration, and the PCB test fixture has been de-embedded. From the results, the efficiency degrades at the lower frequency band, leading to a

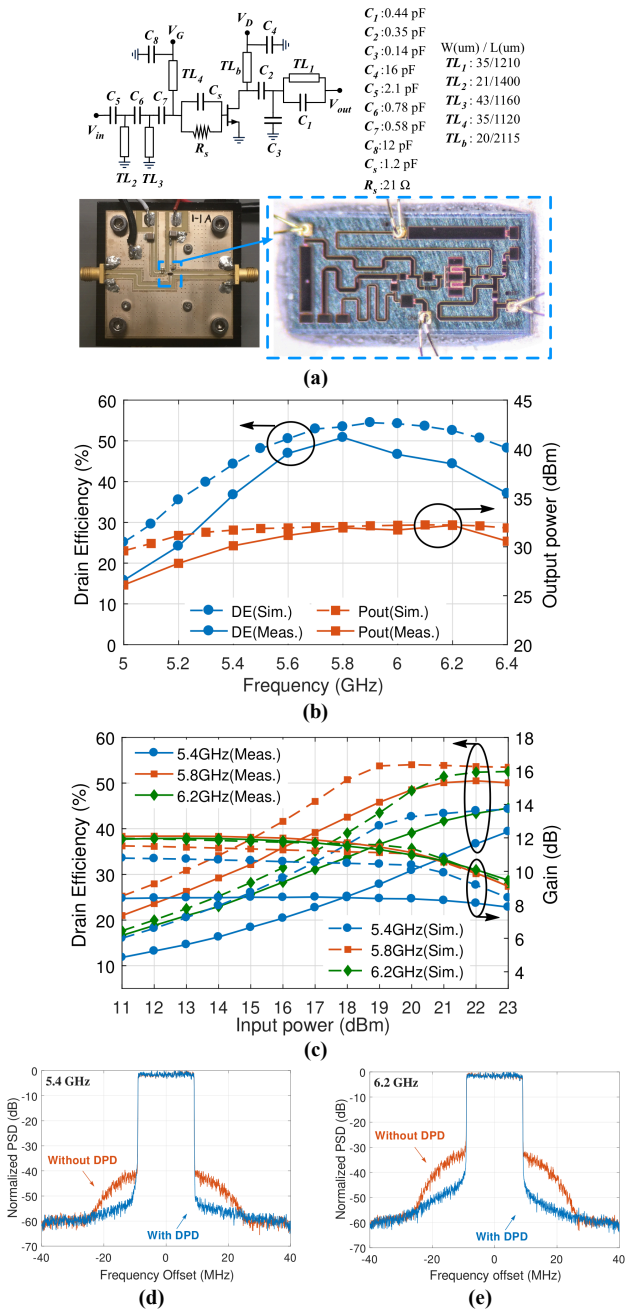

Fig. 4. The proposed circuit structure and the chip photography (a). Measured (b) drain efficiency and output power verses frequency with 22 dBm input power; (c) drain efficiency and gain verses input power across the bandwidth; Spectra plots with 20 MHz LTE signal with and without DPD at (d) 5.4 GHz (e) 6.2 GHz.

reduction in bandwidth. The deviation of measurement results from simulation is mainly due to real circuits implementation and MMIC fabrication variations. Measured highest drain efficiency can reach 50.82% at 5.8 GHz and over 36.8% drain efficiency can be obtained from 5.4 GHz to 6.4 GHz. Measured gain can reach 10.19 dB at 6.2 GHz, and more than 8.5 dB gain is achieved from 5.4 GHz to 6.4 GHz.

The modulated signal measurements were performed inside the available measured bandwidth with a 20 MHz LTE signal

TABLE 2
COMPARISON WITH OTHER C-BAND MMIC GAN PAS

Ref.	Architecture	Technology	Frequency (GHz)	PAE (%)	Psat. (dBm)	Gain (dB)	Size (mm^2)
[21]	Doherty	0.25-μm GaN HEMT	4.5-5.2	45-51	41.2	11.6	4.6
[22]	Harmonic matching	0.25-μm GaN HEMT	4.9-5.9	45.9-61.3	35-36.2	9.8	2.42
[23]	Two-stage	0.25-μm GaN HEMT	5.2-6.8	51.5-56	45.7-46.4	22	12.54
This Work	Continuous Class-B	0.25-μm GaN HEMT	5.4-6.4	32-45.8	30.5-32	8.5-10.19	2

under 12 dBm input signal. Fig. 4(d) and Fig.4 (e) show the output spectrum for 5.4 GHz and 6.2 GHz carrier before and after digital predistortion (DPD). The adjacent channel power ratio (ACPR) is lower than -50 dBc after DPD at 5.4 GHz, ACPR at 6.2 GHz is slightly higher but remains -45 dBc.

The state-of-the-art comparison is shown in Table 2. The proposed PA has small size and is operated at relatively higher frequencies with comparable bandwidth. The efficiency performance may need be further improved. Most publications using different architectures that are either involving higher harmonic control or adopting larger transistor size for better output matching and all of them involve complicated design process. In this paper, we demonstrated, *for the first time*, how to construct matching networks for continuous mode PAs by directly utilizing the special characteristics of *LC* resonance circuits without complex mathematical circuit synthesis. It provides a simple and alternative approach for PA designers in MMIC implementation.

IV. CONCLUSION

A new methodology for constructing broadband continuous mode PA output matching networks was presented. A GaN MMIC PA was fabricated, and the experimental results show maximum 50.82% drain efficiency and 10.19 dB gain were obtained. Various matching networks can be generated by using the proposed procedures, and those can be applied to any other frequencies in different designs.

REFERENCES

[1] Cripps S, Tasker P, Clarke A, Lees J, Benedikt J. On the Continuity of High Efficiency Modes in Linear RF Power Amplifiers. *IEEE Microw. Wireless Compon. Lett.* 2009; 19(10): 665-667.

[2] Carrubba V. Novel Highly Efficient Broadband Continuous Power Amplifier Modes. Ph.D. Cardiff University, Cardiff; 2012.

[3] Tuffy N, Guan L, Zhu A, Brazil TJ. A Simplified Broadband Design Method-ology for Linearized High-Efficiency Continuous Class-F Power Amplifiers. *IEEE Trans. Microw. Theory Tech*. 2012; 60(6): 1952-1963.

[4] Zheng SY, Liu ZW, Zhang XY, Zhou XY, Chan WS. Design of Ultrawideband High Efficiency Extended Continuous Class-F Power Amplifier. *IEEE Trans. Ind. Electron.* 2018; 65(6): 4661-4669.

[5] You F, Li C, Peng J, He S. Design of Broadband High-Efficiency Power Amplifier through Interpolations on Continuous Operation-Modes. *IEEE Access*. 2019; 7: 10663-10671.

[6] Sharma T, Srinidhi ER, Darraji R, et al. High Efficiency Input and Output Harmonically Engineered Power Amplifiers. *IEEE Trans. Microw. Theory Tech*. 2018; 66(2): 1002-1014.

[7] Li Y, Fang X, Jundi A, Huang H, Boumaiza S. Two-Port Network Theory-Based Design Method for Broadband Class J Doherty Amplifiers. *IEEE Access*. 2019; 7: 51028-51038.

[8] Pang J, He S, Huang C, Dai Z, Peng J, You F. A Post-Matching Doherty Power Amplifier Employing Low-Order Impedance Inverters for Broadband Applications. *IEEE Trans. Microw. Theory Tech*. 2015; 63(12): 4061-4071.

[9] Wang J, He S, You F, Shi W, Peng J, Li C. Codesign of High Efficiency Power Amplifier and Ring-Resonator Filter Based on a Series of Continuous Modes and Even–Odd-Mode Analysis. *IEEE Trans. Microw. Theory Tech*. 2018; 66(6): 2867-2878.

[10] Nguyen DP, Pham BL, Pham A. A Compact Ka-Band Integrated Doherty Amplifier With Reconfigurable Input Network. *IEEE Trans. Microw. Theory Tech*. 2019; 67(1): 205-215.

[11] Couturier AM, Poitrenaud N, Serru V, Dionisio R, Fontecavc JJ, Camiade M. 50% High Efficiency X-Band GaN MMIC Amplifier for Space Applications. *Proc. 48th Eur. Microw. Conf*. 2018: 352-355.

[12] Giofrè R, Costanzo F, Sotgia M, Cirillo M, Limiti E. A GaN MMIC HPA with 50W Output Power and 50% PAE for S-Band Radar Systems. *14th European Microwave Integrated Circuits Conference (EuMIC)*. 2019:232-235.

[13] Li S, Hsu SSH, Zhang J, Huang K. Design of a Compact GaN MMIC Doherty Power Amplifier and System Level Analysis With X-Parameters for 5G Communications. *IEEE Trans. Microw. Theory Tech*. 2018; 66(12): 5676-5684.

[14] Duffy MR, Lasser G, Nevett G, Roberg M, Popović Z. A Three-Stage 18.5-24-GHz GaN-on-SiC 4 W 40% Efficient MMIC PA. *IEEE J. of Solid-State Circuits*. 2019;54(9): 2402-2410.

[15] Colantonio P, Giannini F, Leuzzi G, Limiti E. Multiharmonic Manipula-tion for Highly Efficient Microwave Power Amplifiers. *Int. J. RF Microw. Comput.-Aided Eng*. 2001; 11(6): 366-384.

[16] Ekhteraei M, Hayati M, Shama F. High-Efficiency Low Voltage Inverse Class-F Power Amplifier Design Based on Harmonic Control Network Analysis. *IEEE Trans. Circuits Syst. I.* 2020; 67(7): 806-814.

[17] Meng X, Yu C, Liu Y, Wu Y. Design Approach for Implementation of Class-J Broadband Power Amplifiers Using Synthesized Band-Pass and Low-Pass Matching Topology. *IEEE Trans. Microw. Theory Tech*. 2017; 65(12): 4984-4996.

[18] Zhuang Y, Fei Z, Chen A, Huang Y, Rabbi K, Zhou J. Design of Multioctave High Efficiency Power Amplifiers Using Stochastic Reduced Order Models. *IEEE Trans. Microw. Theory Tech.* 2018; 66(2): 1015-1023.

[19] Grebennikov A.RF and Microwave Power Amplifier Design. New York, NY, USA: McGraw-Hill. 2005.

[20] Chen P, Xia J, Merrick BM, Brazil TJ. Multiobjective Bayesian Optimization for Active Load Modulation in a Broadband 20-W GaN Doherty Power Amplifier Design. *IEEE Trans. Microw. Theory Tech*. 2017; 65(3): 860-871.

[21] Lv G, Chen W, Liu X, Ghannouchi FM, Feng Z. A Fully Integrated C-Band GaN MMIC Doherty Power Amplifier With High Efficiency and Compact Size for 5G Application. *IEEE Access*.2019; 7: 71665 - 716741.

[22] Liu B, Mao M, Khanna D, Choi P, Boon CC, Fitzgerald EA. A Highly Efficient Fully Integrated GaN Power Amplifier for 5-GHz WLAN 802.11acApplication. *IEEE Microw. Wireless Compon. Lett.* 2018; 28(5): 437-439.

[23] Noh YS, Yom IB. Highly Integrated C-Band GaN High Power Amplifier MMIC for Phased Array Applications. *IEEE Microw. Wireless Compon. Lett.* 2015; 25(6): 406-408.